Analytical method of calculating the electromagnetic field and power losses in ferromagnetic halfspace, taking into account saturation and hysteresis

J.F. Gieras, M.Sc., Ph.D.

Indexing terms: *Electromagnetic fields, Magnetic permeability, Eddy-current losses, Magnetic materials, Magnetic hysteresis*

Abstract

The steady-state solution of electromagnetic-field problems in ferromagnetic materials is given. The effects of magnetic saturation and hysteresis are included. The solution is based on the differential diffusion equation assuming variable complex magnetic permeability. A precise formula is given to calculate the total power losses due to eddy currents and hysteresis. Computed curves, together with measured curves, are given for active and reactive losses in mild steel. Good agreement is obtained between measured and computed values.

List of principal symbols

a_R = coefficient of active power loss and resistance, taking into account the variable magnetic permeability and hysteresis
a_X = coefficient of reactive power loss and reactance taking into account the variable magnetic permeability and hysteresis
B_m = peak magnetic flux density, T
d = depth of penetation, m
E_m = peak electric field strength, V/m
H_m = peak magnetic field strength, A/m
H_{mcr} = critical magnetic field strength, A/m
m_1, m_2, n = parameters defining the nonlinearity of magnetisation curves
$r_{1,2}$ = roots of characteristic equation for fictitious medium I
$S_z = p + jq$ = normal component of Poynting vector, VA/m^2
t_1, t_2, t_{2max} = parameters expressing variations of the magnetic permeability μ_r and angle ψ with the z-axis
$v_{1,2}, v_{1,2max}$ = roots of characteristic equation for fictitious medium II
z_m, z_p, z_{pmax} = thicknesses of fictitious media I and II, m
μ = magnetic permeability (μ_r = relative, μ_e = equivalent, μ_{ri} = relative initial, μ_{rmax} = relative maximum)
σ = electric conductivity, S/m
ψ = hysteresis angle (ψ_{in} = initial, ψ_{max} = maximum), rad
ω = $2\pi f$ = angular frequency, rad/s
subscript s = surface value

1 Introduction

The diffusion of electromagnetic fields into solid ferromagnetic conductors is an important problem in the design and operation of power apparatus such as electrical machines, transformers and electromagnets. A precise solution for the electromagnetic field in solid iron is difficult, owing to the complicated relationship of magnetic field strength H and flux density B. In general, if saturation or hysteresis are included, the problem becomes intractable by analytical solutions, and only numerical solutions are feasible using the digital computers.[1,2,3]

One-dimensional finite-difference methods are readily able to solve this problem even with modest computer equipment. On the other hand, to understand the numerical methods better, we can first solve Maxwell's equations in ferromagnetic material analytically using an approximate procedure. An analytical approach could be helpful in setting up numerical solutions for electromagnetic field in electrical machines and transformers. As it is known, numerical methods taking into account the variable permeability are still too inefficient from the computation point of view in computer aided design of electrical machines, e.g. linear induction motors with the ferromagnetic secondary and rotary induction motors with solid ferromagnetic rotor. The use of coefficients obtained from analytical methods taking into account saturation and hysteresis considerably reduces the time needed for design with the aid of digital computers.

The most popular approximate methods of electromagnetic field analysis in ferromagnetic materials are the following: Rosenberg's,[4] Haberlands[5,6] enlarged by Agarwal,[7] Nejman's,[8] Kesavamurthy's and Rajagopalan's.[9] These methods can be applied only in some intervals of magnetic field strength and determined conditions. Moreover, these methods are not useful for precise calculation of power losses.

Recently, the problem of saturation and hysteresis was considered analytically, among others, by Heller and Sarma,[10] Barth[11] and O'Kelly.[12] Heller and Sarma[10] investigated the electromagnetic phenomena in ferromagnetic bodies placed in a sinusoidal field under the assumption of an ideal rectangular B/H curve. Barth[11] represented the electromagnetic field in solid iron by complex Fourier series, the coefficients of which may be calculated by harmonic analysis of measured static hysteresis loops. O'Kelly[12] gave a solution for the electromagnetic field in solid iron including both hysteresis and eddy currents effects by considering only fundamental harmonics of flux density and magnetic-field strength expressed in terms of phasor vectors. Hysteresis in ferromagnetic material is represented by an idealised elliptical B/H curve.

The purpose of this paper is to give one more analytical method, which can be applied in a wide variation range of magnetic field strength, theoretically from zero to infinity.

2 Assumptions

The analysis of electromagnetic field in solid ferromagnetic material will be carried out with the following assumptions:

(*a*) the thickness of ferromagnetic body far exceeds the depth of penetration, so that the body can be developed to correspond to an infinite halfspace
(*b*) the radius of curvature of the halfspace far exceeds the depth of penetration, so that analysis can be made in the Cartesian-coordinate system
(*c*) the incident electromagnetic wave is plane polarised, i.e. the magnetic component H_{my} is in the y-direction, the electric component E_{mx} is in the x-direction and the z-axis is chosen normal to the surface and extends into the material
(*d*) the magnetic field strength H_{msy} at the surface of ferromagnetic halfspace is known
(*e*) the electric conductivity is independent of temperature variation inside the halfspace body
(*f*) the anisotropy of ferromagnetic halfspace is neglected
(*g*) all the field quantities vary in time according to the sinusoidal law
(*h*) the higher harmonics of magnetic and electric field strength are omitted.

Assumptions (*g*) and (*h*) can be set up because in relation to fundamental harmonic the higher harmonics are more strongly damped inside halfspace body.

Paper 7950 S, first received 19th January and in revised form 10th June 1977

Dr. Gieras is with the Department of Electrical Engineering, Technical University of Poznań, Poznań, Poland

3 General equations of one-dimensional electromagnetic field in ferromagnetic material

In the ferromagnetic material both amplitude and phase angle of magnetic flux density depend on magnetic field strength. Let us consider the magnetic flux density B varying sinusoidally in time, i.e. $B(z, t) = B_m(z) \exp(j\omega t)$. The first harmonic of magnetic field strength leads the magnetic flux density by hysteresis angle $\psi(z)$, i.e.. $H(z, t) = H_m(z) \exp\{j[\omega t + \psi(z)]\}$. At an arbitrary point z, the correlation between magnetic flux density and magnetic field strength can be expressed with the aid of complex magnetic permeability:

$$\mu(z) = \frac{B_m(z)}{H_m(z)} \exp[-j\psi(z)] = \mu_0 \mu_r(z) \exp[-j\psi(z)] \quad (1)$$

Values of relative magnetic permeability $\mu_r = f(H_m)$ and hysteresis angle $\psi = f(H_m)$ of various types of carbon steel are given in Table 1.

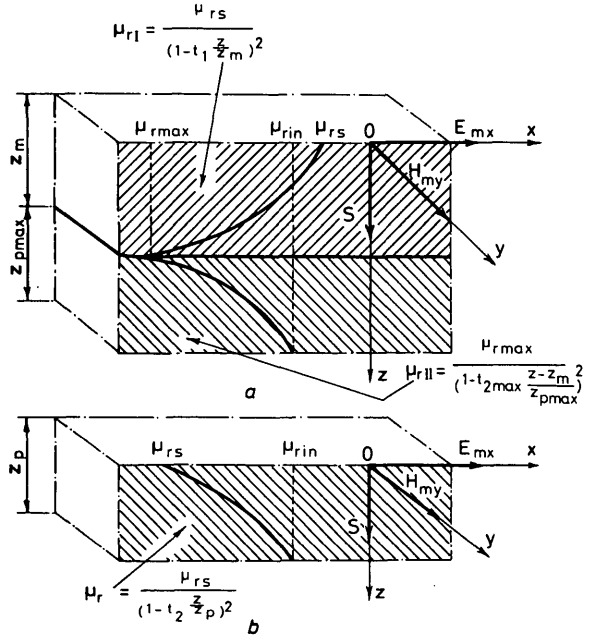

Fig. 1
Ferromagnetic halfspace in one-dimensional electromagnetic field

a Variation of relative magnetic permeability μ_r with the z axis in the case of $H_{msy} > H_{mcr}$
b Variation of relative magnetic permeability μ_r with the z axis in the case of $H_{msy} \leqslant H_{mcr}$

The complex magnetic permeability $\mu(z)$ will be introduced into Maxwell's equations. For conducting homogeneous and isotropic ferromagnetic material, the Maxwell's equations with displacement currents and convection currents assumed to be negligible and all field quantities varying sinusoidally in time are as follows:

$$\frac{\partial^2 H_m(z, t)}{\partial z^2} = j\omega\sigma B_m(z, t) \quad (2)$$

$$E_m(z, t) = -\frac{1}{\partial} \frac{\partial H_m(z, t)}{\partial z} \quad (3)$$

At the power frequencies, i.e. 50 or 60 Hz, the displacement currents and convection currents can be omitted. Eqn. 2 is also called the diffusion equation.

It is necessary to introduce into eqn. 2 such an approximation of complex magnetic permeability varying with the z coordinate that the nonlinear eqn. 2 can be solved from the mathematical points of view.

4 Magnetic permeability and hysteresis angle

Magnetic field penetrating into a ferromagnetic material decays monotonically along the z-axis. At some depth its value is equal to zero. The variations of relative permeability μ_r and angle ψ with the z axis can be foreseen on the basis of magnetisation curves $\mu_r = f(H_m)$ and $\psi = f(H_m)$. Magnetic field strength corresponding to maximum permeability μ_{rmax} will be called the critical magnetic field strength H_{mcr}. If the magnetic field strength H_{ms} at the surface of ferromagnetic medium is higher than the critical field strength H_{mcr}, then the relative permeability μ_r and angle ψ increase from the surface values to the maximum ones (for $H_m = H_{mcr}$). Subsequently, μ_r and ψ decrease from the maximum values to the initial ones (for $H_m = 0$) at a depth where magnetic field strength is equal to zero. Thus, for high magnetic saturation $H_{ms} > H_{mcr}$, the variation of relative permeability μ_r with the z axis shows that it is possible to replace the ferromagnetic halfspace by two fictitious nonlinear media with finite thicknesses in such a way that:

(i) in the outer medium I (Fig. 1*a*) with its thickness z_m and parameters σ, $\mu_{rI} = f(z)$, $\psi_I = f(z)$ relative magnetic permeability and angle ψ_I increase monotonically from surface values for $H_m = H_{ms}$ to maximum ones for $H_m = H_{mcr}$

(ii) in the inner medium II (Fig. 1*a*) with its thickness z_{pmax} and parameters σ, $\mu_{rII} = f(z)$, $\psi_{II} = f(z)$ relative magnetic permeability and angle ψ_{II} decrease monotonically from maximum for $H_m = H_{mcr}$ to initial values for $H_m = 0$.

The thickness z_m of a fictitious outer medium I depends on magnetic field strength H_{ms} at the surface. For the given type of steel and determined frequency, the thickness z_{pmax} of a fictitious inner medium II is independent of the surface magnetic field strength. We can assume that in the outer medium I, i.e. for $H_{ms} > H_{mcr}$ relative

Table 1
MAGNETIC AND ELECTRIC PROPERTIES OF TESTED SAMPLES OF CARBON STEEL

Number of sample	Chemical composition	Magnetisation curves $\mu_r = f(H_m)$ and $\psi = f(H_m)$ 100 A/m H_{mcr}		5000 A/m		20000 A/m		Electric conductivity at 293·2 K S/m	H_{mcr} A/m
		μ_r	ψ rad	μ_r	ψ rad	μ_r	ψ rad		
1	0·27% C, 0·70% Mn, 0·12 – 0·30% Si, 0·050% P, 0·055% S	130	0·314	1500	0·838	240	0·14	70	0·052	6.20×10^6	350
2	0·32 – 0·40% C, 0·50 – 0·80% Mn, 0·17 – 0·37% Si, 0·25% Cr, 0·25% Ni, 0·25% Cu, 0·040% P, 0·040% S	90	0·192	640	0·803	220	0·332	70	0·14	4.50×10^6	800
3	0·52 – 0·60% C, 0·50 – 0·80% Mn, 0·17 – 0·37% Si, 0·25% Cr, 0·25% Ni, 0·25% Cu, 0·040% P, 0·040% S	70	0·140	535	0·768	215	0·314	70	0·14	4.64×10^6	900
4	0·62 – 0·70% C, 0·50 – 0·80% Mn, 0·17 – 0·37% Si, 0·25% Cr, 0·25% Ni, 0·25% Cu, 0·040% P, 0·040% S	40	0·087	430	0·716	200	0·297	70	0·14	4.57×10^6	1150

magnetic permeability and angle ψ_I change in the z direction, according to the following formulas:

$$\mu_{rI} = \frac{\mu_{rs}}{\left(1 - t_1 \frac{z}{z_m}\right)^2} \tag{4}$$

$$\psi_I = \frac{\psi_s}{\left(1 - t_1 \frac{z}{z_m}\right)^2} \tag{5}$$

The parameter $t_1 = f(H_{ms})$ has to remain within $0 < t_1 < 1$. It cannot take the value $t_1 = 1$ because, in this case, the values μ_{rI} and ψ_I for $z = z_m$ would tend to infinity. The parameter

$$t_1 = 1 - \left(\frac{\mu_{rs}}{\mu_{rmax}}\right)^{1/2} \simeq 1 - \left(\frac{\psi_s}{\psi_{max}}\right)^{1/2} \tag{6}$$

can be determined from the conditions $\mu_{rI} = \mu_{rmax}$ and $\psi_I = \psi_{max}$ in the depth $z = z_m$.

Similarly, in the inner medium II, i.e. in unsaturated region, we can assume that relative magnetic permeability and angle ψ_{II} change according to the formulas:

$$\mu_{rII} = \frac{\mu_{rmax}}{\left(1 - t_{2\,max} \frac{z - z_m}{z_{p\,max}}\right)^2} \tag{7}$$

$$\psi_{II} = \frac{\psi_{max}}{\left(1 - t_{2\,max} \frac{z - z_m}{z_{p\,max}}\right)^2} \tag{8}$$

where parameter $t_{2\,max} < 0$ is equal to

$$t_{2\,max} = 1 - \left(\frac{\mu_{rmax}}{\mu_{rin}}\right)^{1/2} \simeq 1 - \left(\frac{\psi_{max}}{\psi_{in}}\right)^{1/2} \tag{9}$$

However, if the magnetic field strength H_{ms} at the surface of ferromagnetic medium is less than or equal to critical field strength, then relative magnetic permeability and angle ψ decrease monotonically from surface values (for $H_m = H_{ms}$) to the initial ones (for $H_m = 0$). Thus, in the case of low magnetic saturation ($H_{ms} \leqslant H_{mcr}$), the ferromagnetic halfspace can be replaced by a single layer with its thickness z_p and parameters σ, $\mu_r = f(z)$ and $\psi = f(z)$. Instead of parameter $t_{2\,max}$, we have to put into eqns. 7 and 8 the parameter

$$t_2 = 1 - \left(\frac{\mu_{rs}}{\mu_{rin}}\right)^{1/2} \simeq 1 - \left(\frac{\psi_s}{\psi_{in}}\right)^{1/2} \tag{10}$$

In this case, the magnetic permeability and hysteresis angle change according to the following eqns. (Fig. 1*b*):

$$\mu_r = \frac{\mu_{rs}}{\left(1 - t_2 \frac{z}{z_p}\right)^2} \tag{11}$$

$$\psi = \frac{\psi_s}{\left(1 - t_2 \frac{z}{z_p}\right)^2} \tag{12}$$

Expressions for complex magnetic permeability in cases of high and low magnetic saturation are given in Appendix 9.1.

5 Solution of diffusion equation

On assumptions given in section 2, exprs. 1, 4, 5, 7 and 8 and Appendixes 9.1 and 9.2, the solutions of one-dimensional electromagnetic field eqns. 2 and 3 in the case of $H_{msy} > H_{mcr}$ are as follows:

(i) for $0 \leqslant z \leqslant z_m$

$$H_{myI} = \frac{1}{M}\left[A \exp(r_1 \zeta_1) + B \exp(r_2 \zeta_1)\right] H_{msyI} \tag{13}$$

$$E_{mxI} = \frac{t_1}{z_m \sigma} \frac{1}{M} \{r_1 A \exp[(r_1 - 1)\zeta_1] + r_2 B \exp[(r_2 - 1)\zeta_1]\} H_{msyI} \tag{14}$$

(ii) for $z_m \leqslant z \leqslant z_m + z_{p\,max}$

$$H_{myII} = \frac{1}{M} \frac{t_1}{z_m} (r_1 - r_2) \exp[(r_1 + r_2 - 1)\beta] H_{msyI} \exp(v_{2\,max}\zeta_{2\,max}) = H_{mcr} \exp(v_{2\,max}\zeta_{2\,max}) \tag{15}$$

$$E_{mxII} = \frac{t_{2\,max} v_{2\,max}}{z_{p\,max}\sigma} \frac{1}{M} \frac{t_1}{z_m} \times (r_1 - r_2) \exp[(r_1 + r_2 - 1)\beta] H_{msyI} \exp[(v_{2\,max} - 1)\zeta_{2\,max}] = \frac{t_{2\,max} v_{2\,max}}{z_{p\,max}\sigma} H_{mcr} \exp[(v_{2\,max} - 1)\zeta_{2\,max}] \tag{16}$$

where

$$A = \left[\frac{t_{2\,max} v_{2\,max}}{z_{p\,max}} - \frac{t_1 r_2}{z_m} \exp(-\beta)\right] \exp(r_2 \beta)$$

$$B = \left[\frac{t_1 r_1}{z_m} \exp(-\beta) - \frac{t_{2\,max} v_{2\,max}}{z_{p\,max}}\right] \leqslant \exp(r_1 \beta)$$

$$M = A + B$$

$$\zeta_1 = \ln\left(1 - t_1 \frac{z}{z_m}\right)$$

$$\zeta_{2\,max} = \ln\left(1 - t_{2\,max} \frac{z - z_m}{z_{p\,max}}\right)$$

$$\beta = \ln(1 - t_1)$$

$$r_1 = r_1' + j r_1'' = \frac{2}{m_1} + j \frac{4 - m_1}{2m_1} \left\{1 - \left(\frac{\bar{m}_1}{4 - m_1}\right)^2 \left[1 + 8\left(\frac{z_m}{d_s t_1}\right)^2 \sin\frac{\psi_s}{1 - t_1}\right]\right\}^{1/2} \tag{17}$$

$$r_2 = r_2' + j r_2'' = \frac{2}{m_2} + j \frac{4 - m_2}{2m_2} \left\{1 - \left(\frac{m_2}{4 - m_2}\right)^2 \left[1 + 8\left(\frac{z_m}{d_s t_1}\right)^2 \sin\frac{\psi_s}{1 - t_1}\right]\right\}^{1/2} \tag{18}$$

$$v_{2\,max} = v_{2\,max}' + j v_{2\,max}'' = \frac{2}{n} + j \frac{4 - n}{2n} \left\{1 - \left(\frac{n}{4 - n}\right)^2 \left[1 + 8\left(\frac{z_{p\,max}}{d_{max} t_{2\,max}}\right)^2 \sin\frac{\psi_{max}}{1 - t_{2\,max}}\right]\right\}^{1/2} \tag{19}$$

$$z_m = \frac{d_s t_1 (4 - m_1)}{2m_1 \cos\frac{\psi_s}{1 - t_1}} \left\{\left[1 - \left(\frac{m_1}{4 - m_1}\right)^2\right]^{1/2} \left[\cos\frac{\psi_s}{1 - t_1}\right]^{1/2} - \sin\frac{\psi_s}{1 - t_1}\right\}^{1/2} \tag{20}$$

$$z_{p\,max} = \frac{d_{max} t_{2\,max} (4 - n)}{2n \cos\frac{\psi_{max}}{1 - t_{2\,max}}} \left\{\left[1 - \left(\frac{n}{4 - n}\right)^2\right]^{1/2} \left[\cos\frac{\psi_{max}}{1 - t_{2\,max}}\right]^{1/2} - \sin\frac{\psi_{max}}{1 - t_{2\,max}}\right\}^{1/2} \tag{21}$$

The parameters m_1, m_2, n come from equations of magnetisation curves (Appendix 9.2).

For the magnetic permeability μ_{rs} at the surface of medium I, the depth of penetration d_s of electromagnetic wave is equal to

$$d_s = \left(\frac{2}{\omega \mu_0 \mu_{rs} \sigma}\right)^{1/2} \tag{22}$$

To calculate the depth of penetration d_{max} for medium II we have to replace the permeability μ_{rs} by the maximum permeability μ_{rmax}, i.e.

$$d_{max} = \left(\frac{2}{\omega \mu_0 \mu_{rmax} \sigma}\right)^{1/2} \tag{23}$$

In the case of $H_{msy} \leqslant H_{mcr}$, eqns. 2 and 3 can be solved in the same way. We obtain

$$H_{my} = H_{msy} \exp(v_2 \zeta_2) \tag{24}$$

$$E_{mx} = \frac{t_2 v_2}{z_p \sigma} H_{msy} \exp[(v_2 - 1)\zeta_2] \tag{25}$$

where

$$\zeta_2 = \ln\left(1 - t_2 \frac{z}{z_p}\right)$$

$$v_2 = v_2' + jv_2'' =$$

$$= \frac{2}{n} + j\frac{4-n}{2n}\left\{1 - \left(\frac{n}{4-n}\right)^2 \times \left[1 + 8\left(\frac{z_p}{d_s t_2}\right)^2 \sin\frac{\psi_s}{1-t_2}\right]\right\}^{1/2} \quad (26)$$

$$z_p = \frac{d_s t_2 (4-n)}{2n \cos\frac{\psi_s}{1-t_2}}\left\{\left[1 - \left(\frac{n}{4-n}\right)^2\right] \cos\frac{\psi_s}{1-t_2}\right]^{1/2} - \sin\frac{\psi_s}{1-t_2}\Bigg\}^{1/2} \quad (27)$$

From the mathematical point of view, the solution of diffusion eqn. 2 is discussed in Appendixes 9.3 and 9.4.

6 Power loss density

The energy flux density is determined by the normal component of Poynting vector in the symbolic form

$$S_z = \tfrac{1}{2}(E_{mx} H_{my}^*)_{z=0} = p + jq \quad (28)$$

where H_{my}^* is the conjugate of H_{my} in eqn. 13 or 24. Substituting eqns. 13 and 14 or 24 and 25 into eqn. 28 we obtain

(i) for high magnetic saturation $H_{msy} > H_{mcr}$

$$S_z = \frac{t_1}{z_m \sigma}\frac{1}{|M|^2}(r_1 A + r_2 B)(A^* + B^*)\frac{|H_{msy}|^2}{2} \quad (29)$$

(ii) for unsaturated ferromagnetic material, i.e. $H_{msy} \leqslant H_{mcr}$

$$S_z = \frac{t_2 v_2}{z_p \sigma}\frac{|H_{msy}|^2}{2} \quad (30)$$

Eqns. 29 and 30 can be transformed into the form

$$S_z = p + jq = (a_R + j a_X)\frac{1}{d_s \sigma}\frac{|H_{msy}|^2}{2} \quad (31)$$

where:

(i) for $H_{msy} > H_{mcr}$

$$a_R = \frac{d_s t_1}{z_m}\,\mathrm{Re}\,\frac{r_1 A + r_2 B}{A + B} \quad (32)$$

$$a_X = \frac{d_s t_1}{z_m}\,\mathrm{Im}\,\frac{r_1 A + r_2 B}{A + B} \quad (33)$$

(ii) for $H_{msy} \leqslant H_{mcr}$

$$a_R = \frac{d_s t_2}{z_p} v_2' \quad (34)$$

$$a_X = \frac{d_s t_2}{z_p} v_2'' \quad (35)$$

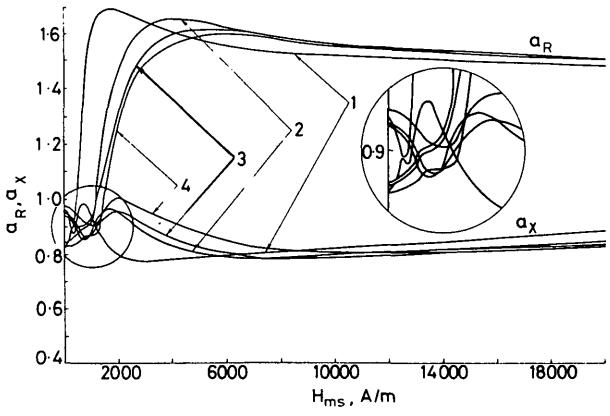

Fig. 2
Coefficients of active power losses $a_R = f(H_{ms})$ and reactive power losses $a_X = f(H_{ms})$ for carbon steel given in Table 1

Coefficients a_R, a_X depend only on magnetic properties of ferromagnetic material represented by parameters $m_1, m_2, n, \mu_{rs}, \mu_{rmax}, \psi_s, \psi_{max}$ and are independent of frequency. Values of coefficients a_R and a_X are determined for four types of carbon steel (Table 1). The magnetic permeability and hysteresis angle of steel given in Table 1 were measured using rotative ellipsoids, like shaped samples. The calculation results of coefficients a_R, a_X are shown on graphs in Fig. 2. To verify eqn. 31, the active- and reactive-power losses in the

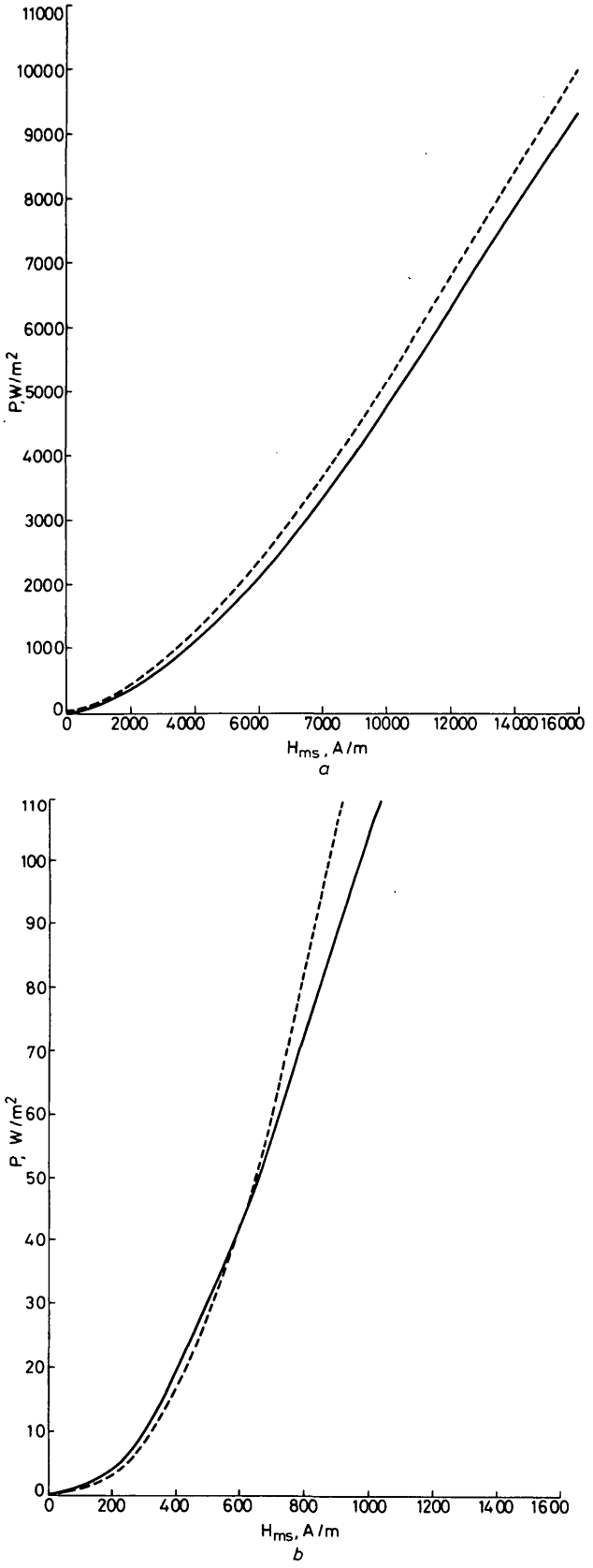

Fig. 3
Active power losses at the frequency 50 Hz in carbon steel containing 0·27% carbon (Table 1)

a For the case of high magnetic saturation
b For the case of low magnetic saturation
——— measured curves
------ calculated curves

carbon steel containing 0·27% carbon (Table 1) have been measured. The tests were performed using wattmeter method[11] on a solid annular steel sample with the following data: outer diameter = 0·1591 m, inner diameter = 0·1404 m, thickness = 0·196 m. The ring was furnished with evenly distributed copper windings: primary coil = 156 turns, secondary coil = 156 turns. At the frequency 50 Hz the active-power losses calculated on the basis of eqns. 31, 32 and 34 and measured-power losses are shown in Fig. 3. The reactive-power losses at the frequency 50 Hz calculated in terms of eqns. 31, 33 and 35 and measured-power losses are shown in Fig. 4. The comparison of the measured and calculated curves shows the validity of the assumptions and analysis presented here.

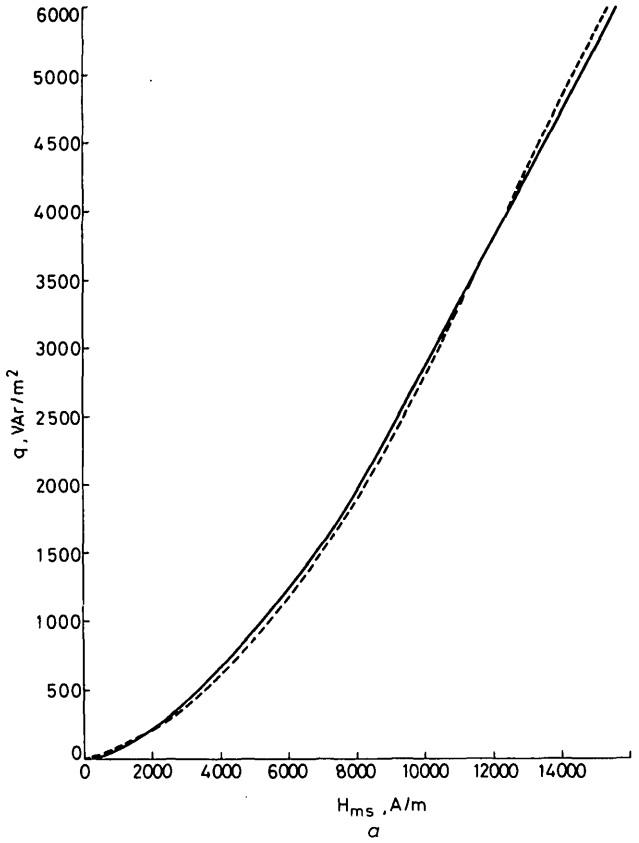

Fig. 4
Reactive power losses at the frequency 50 Hz in carbon steel containing 0·27% carbon (Table 1)

a For the case of high magnetic saturation
b For the case of low magnetic saturation
——— measured curves
------ calculated curves

7 Conclusion

The analytical method worked out here, which is taking into account saturation and hysteresis is a correct one. In the case of reactive-power losses (Fig. 4) this method is more precise than in case of active-power losses (Fig. 3). For the ferromagnetic medium the Maxwell's equations can be solved in the same way when μ_r = a constant and ψ = a constant if one introduces equivalent complex magnetic permeability

$$\mu_{re} = \mu_{rs}(\mu' - j\mu'') \tag{36}$$

where

$$\mu' = a_R a_X$$

and

$$\mu'' = \tfrac{1}{2}(a_R^2 - a_X^2)$$

It is possible to apply this equivalent permeability to 2-dimensional and 3-dimensional field problems, e.g. in linear induction motors with the ferromagnetic secondary, or ferromagnetic tanks of transformers.

8 References

1 GILLOT, D.H., and CALVERT, J.F.: 'Eddy-current loss in saturated solid magnetic plates, rods and conductors,' *IEEE Trans.*, 1965, **MAG-1**, pp. 126–137
2 LIM, K.K., and HAMMOND, M.: 'Numerical method for determining electromagnetic field in saturated steel plates,' *Proc. IEE*, 1972, **119**, (11), pp. 1667–1674
3 ZAKRZEWSKI, K., and PIETRAS, F.: 'Method of calculating the electromagnetic field and power losses in ferromagnetic materials, taking into account magnetic hysteresis', *ibid.*, 1971, **118**, (11), pp. 1679–1685
4 ROSENBERG, E.: 'Wirbelströme in massiven Eisen', *ETZ*, 1923, **22**, pp. 513–518
5 HABERLAND, F.: 'Theorie des magnetischen Wechselfeldes im Luftspalt von massiven Eisen', *Archiv für Elektrotechnik*, 1934, **28**, pp. 234–246
6 HABERLAND, G., and HABERLAND, F.: 'Das Wechselfeldes im gesattigen massiven Eisen', *ibid.*, 1936, **30**, pp. 126–133
7 AGARWAL, P.D.: 'Eddy current losses in solid and laminated iron', *AIEE, Trans.*, 1959, **CE-78**, pp. 169–181
8 NEJMAN, L.R.: 'Povierchnostnyj effiekt v ferromagnitnych tielach', GEI, Leningrad-Moskva, 1949
9 KESAVAMURTHY, N., and RAJAGOPALAN, P.K.: 'An analytical method taking account of saturation and hysteresis for calculating the iron loss in solid-iron cores subjected to an alternating field', *Proc. IEE*, 1961, **108C**, pp. 237–243
10 HELLER, B., and SARMA, M.S.R.: 'The electromagnetic field in solid iron', *Acta Tech. CSAV*, 1968, 6, pp. 735–753
11 BARTH, J.B.: 'Alternating electromagnetic field, eddy currents and power loss in solid iron', *Proc. IEE*, 1973, **120**, (11), pp. 1454–1461
12 O'KELLY, D.: 'Flux penetration and core loss in solid iron', *IEEE Trans.*, 1975, **MAG-11**, (1), pp. 55–60

9 Appendixes

9.1 Complex magnetic permeability

Variable hysteresis losses in the z direction are approximately equal to the losses for the mean angle ψ within $0 \leqslant z \leqslant z_m$, $z_m \leqslant z \leqslant z_m + z_{pmax}$, or $0 \leqslant z \leqslant z_p$.

Introducing eqns. 4 and 5, or eqns. 7 and 8 into expr. 1, in case of high magnetic saturation we obtain:

(i) for $0 \leqslant z \leqslant z_m$

$$\mu_{\mathrm{I}}(z) = \frac{\mu_0 \mu_{rs}}{\left(1 - t_1 \dfrac{z}{z_m}\right)^2} \exp\left[-j \frac{\psi_s}{\left(1 - t_1 \dfrac{z}{z_m}\right)^2}\right] \simeq \frac{\mu_0 \mu_{rs}}{\left(1 - t_1 \dfrac{z}{z_m}\right)^2} \left(\cos \frac{\psi_s}{1 - t_1} - j \sin \frac{\psi_s}{1 - t_1}\right) \tag{37}$$

(ii) for $z_m \leqslant z \leqslant z_m + z_{pmax}$

$$\mu_{\mathrm{II}}(z) = \frac{\mu_0 \mu_{rmax}}{\left(1 - t_{2\,max} \dfrac{z - z_m}{z_{pmax}}\right)^2} \exp\left[-j \frac{\psi_{max}}{\left(1 - t_{2\,max} \dfrac{z - z_m}{z_{pmax}}\right)^2}\right]$$

$$\simeq \frac{\mu_0\mu_{rmax}}{\left(1-t_{2\,max}\dfrac{z-z_m}{z_{pmax}}\right)^2}$$

$$\left(\cos\frac{\psi_{max}}{1-t_{2\,max}} - j\sin\frac{\psi_{max}}{1-t_{2\,max}}\right) \quad (38)$$

Introducing eqns. 11 and 12 into expr. 1, in the case of unsaturated ferromagnetic material we have:

$$\mu(z) = \frac{\mu_0\mu_{rs}}{\left(1-t_2\dfrac{z}{z_p}\right)^2}\exp\left[-j\frac{\psi_s}{\left(1-t_2\dfrac{z}{z_p}\right)^2}\right] \simeq$$

$$\frac{\mu_0\mu_{rs}}{\left(1-t_2\dfrac{z}{z_p}\right)^2}\left(\cos\frac{\psi_s}{1-t_2} - j\sin\frac{\psi_s}{1-t_2}\right) \quad (39)$$

Such form of complex magnetic permeability as eqns. 37, 38 and 39 makes it possible to solve eqn. 2.

9.2 Approximation of magnetisation curves

The measured magnetisation curves $\mu_r = f(H_m)$ and $\psi = f(H_m)$ for constructional steel are given in Table 1. These curves can be expressed simply by equation of parabola, e.g. for magnetic permeability

(i) for $H_m > H_{mcr}$

$$\mu_r = a_\mu H_m^{-m_1} \quad (40)$$

(ii) for $H_m \leqslant H_{mcr}$

$$\mu_r = b_\mu H_m^{-m_2} \quad (41)$$

where $m_1 > 0, m_2 < 0$.

Each material will have a characteristic value of m_1 and m_2, which can be determined from its magnetisation curve. Moreover, because of the inflection point of the curve $\mu_r = f(H_m)$ in the unsaturated region it is better to assume the straightline approximation, i.e.

$$\mu_r = c_\mu H_m^{-n} \quad (42)$$

where $n = -1$ for all ferromagnetic materials.

The constants a_μ, b_μ and c_μ are a scale factor which also have characteristic values for a given material.

Eqns. 40 and 42 for constructional steel are shown in Table 2.

Table 2
APPROXIMATION OF MAGNETISATION CURVES OF CARBON STEEL

Number of sample	$H_m > H_{mcr}$ eqn. 40	$H_m \leqslant H_{mcr}$ eqn. 42	Parameters into eqns. 40, 41 and 42		
1 0·27% C	$\mu_r = 7 \times 10^5 H_m^{-0.94}$	$\mu_r = 4{\cdot}3\,H_m$	0·94	−1	−1
2 0·32 – 0·40% C	$\mu_r = 4{\cdot}4 \times 10^5 H_m^{-0.90}$	$\mu_r = 0{\cdot}8\,H_m$	0·90	−1	−1
3 0·52 – 0·60% C	$\mu_r = 2{\cdot}9 \times 10^5 H_m^{-0.85}$	$\mu_r = 0{\cdot}6\,H_m$	0·85	−1	−1
4 0·62 – 0·70% C	$\mu_r = 2{\cdot}6 \times 10^5 H_m^{-0.85}$	$\mu_r = 0{\cdot}6\,H_m$	0·85	−1	−1

9.3 Solution of diffusion equation

In the case of $H_{msy} > H_{mcr}$, equations of one-dimensional electromagnetic field are the following:

(i) for $0 \leqslant z \leqslant z_m$

$$\frac{\partial^2 H_{my\,I}}{\partial z^2} = j\omega\mu_0\sigma\frac{\mu_{rs}}{\left(1-t_1\dfrac{z}{z_m}\right)^2}\left(\cos\frac{\psi_s}{1-t_1} - j\sin\frac{\psi_s}{1-t_1}\right)H_{my\,I} \quad (43)$$

$$E_{mx\,I} = -\frac{1}{\sigma}\frac{\partial H_{my\,I}}{\partial z} \quad (44)$$

(ii) for $z_m \leqslant z \leqslant z_m + z_{pmax}$

$$\frac{\partial^2 H_{my\,II}}{\partial z^2} = j\omega\mu_0\sigma\frac{\mu_{rmax}}{\left(1-t_{2\,max}\dfrac{z-z_m}{z_{pmax}}\right)^2}\left(\cos\frac{\psi_{max}}{1-t_{2\,max}} - j\sin\frac{\psi_{max}}{1-t_{2\,max}}\right)H_{my\,II} \quad (45)$$

$$E_{mx\,II} = -\frac{1}{\sigma}\frac{\partial H_{my\,II}}{\partial z} \quad (46)$$

Putting

$$\exp\zeta_1 = 1 - t_1\frac{z}{z_m} \text{ for } 0 \leqslant z \leqslant z_m$$

and

$$\exp\zeta_{2\,max} = 1 - t_{2\,max}\frac{z-z_m}{z_{pmax}} \text{ for } z_m \leqslant z \leqslant z_m + z_{pmax}$$

differential eqns. 43 and 45 can be transformed into second-order linear equations with constant coefficients

$$\frac{\partial^2 H_{my\,I}}{\partial\zeta_1^2} - \frac{\partial H_{my\,I}}{\partial\zeta_1} + - 2\frac{1}{d_s^2}\left(\sin\frac{\psi_s}{1-t_1} + j\cos\frac{\psi_s}{1-t_1}\right)\left(\frac{z_m}{t_1}\right)^2 H_{my\,I} = 0 \quad (47)$$

$$\frac{\partial^2 H_{my\,II}}{\partial\zeta_{2\,max}^2} - \frac{\partial H_{my\,II}}{\partial\zeta_{2\,max}} + - 2\frac{1}{d_{max}^2}\left(\sin\frac{\psi_{max}}{1-t_{2\,max}} + j\cos\frac{\psi_{max}}{1-t_{2\,max}}\right)\left(\frac{z_{pmax}}{t_{2\,max}}\right)^2 H_{my\,II} = 0 \quad (48)$$

The following characteristic equations correspond to eqns. 47 and 48:

$$r^2 - r - 2\frac{1}{d_s^2}\left(\sin\frac{\psi_s}{1-t_1} + j\cos\frac{\psi_s}{1-t_1}\right)\left(\frac{z_m}{t_1}\right)^2 = 0$$

$$v_{max}^2 - v_{max} - 2\frac{1}{d_{max}^2}\left(\sin\frac{\psi_{max}}{1-t_{2\,max}} + j\cos\frac{\psi_{max}}{1-t_{2\,max}}\right)\left(\frac{z_{pmax}}{t_{2\,max}}\right)^2 = 0$$

with complex roots

$$r_{1,2} = r'_{1,2} + jr''_{1,2} = \tfrac{1}{2}\left(1 \pm \frac{1}{\sqrt{2}}K_s\right) \pm j\frac{1}{2\sqrt{2}}K_s \quad (49)$$

$$v_{1,2\,max} = v'_{1,2\,max} + j\,v''_{1,2\,max} = \tfrac{1}{2}\left(1 \pm \frac{1}{\sqrt{2}}K_{max}\right) \pm j\frac{1}{2\sqrt{2}}K_{max} \quad (50)$$

where

$$K_s = \left\{\left[1 + 16\left(\frac{z_m}{d_s t_1}\right)^2\sin\frac{\psi_s}{1-t_1} + 64\left(\frac{z_m}{d_s t_1}\right)^4\right]^{1/2} + 1 + 8\left(\frac{z_m}{d_s t_1}\right)^2\sin\frac{\psi_s}{1-t_1}\right\}^{1/2}$$

$$K_{max} = \left\{\left[1 + 16\left(\frac{z_{p\,max}}{d_{max}t_{2\,max}}\right)^2 \sin\frac{\psi_{max}}{1-t_{2\,max}} + 64\frac{z_{p\,max}}{d_{max}t_{2\,max}}\right)^4\right]^{1/2} + 1 + 8\left(\frac{z_{p\,max}}{d_{max}t_{2\,max}}\right)^2 \sin\frac{\psi_{max}}{1-t_{2\,max}}\Bigg\}^{1/2}$$

General solutions of the eqns. 43, 44, 45 and 46 have the form:

(i) for $0 \leqslant z \leqslant z_m$

$$H_{myI} = H'_{myI} + H''_{myI} = C_{1yI}\exp(r_1\zeta_1) + C_{2yI}\exp(r_2\zeta_1) \quad (51)$$

$$E_{myI} = \frac{t_1}{z_m\sigma}\{r_1C_{1yI}\exp[(r_1-1)\zeta_1] + r_2C_{2yI}\exp[(r_2-1)\zeta_1]\} \quad (52)$$

(ii) for $z_m \leqslant z \leqslant z_m + z_{p\,max}$

$$H_{myII} = H''_{myII} + H'_{myII} \quad C_{1yII}\exp(v_{1\,max}\zeta_{2\,max}) + C_{2yII}\exp(v_{2\,max}\zeta_{2\,max}) \quad (53)$$

$$E_{mxII} = \frac{t_{2\,max}}{z_{p\,max}\sigma}\{v_{1\,max}C_{1yII}\exp[(v_{1\,max}-1)\zeta_{2\,max}] + v_{2\,max}C_{2yII}\exp[(v_{2\,max}-1)\zeta_{2\,max}]\} \quad (54)$$

The constant $C_{1yII} = 0$ because, in medium II, the reflected wave cannot exist. The remaining constants C_{1yI}, C_{2yI} and C_{2yII} are determined from boundary conditions for $z = 0$ and $z = z_m$.

In the case of $H_{msy} \leqslant H_{mcr}$ the solution of the one-dimensional field problem is similar.

9.4 Determination of quantities $r_{1,2}$, $v_{2\,max}$, v_2, z_m, $z_{p\,max}$ and z_p

Introducing magnetisation curve approximations 40, 41 and 42 into eqns. 4 and 7 in the case of $H_{msy} > H_{mcr}$ we obtain the following equations:

(i) for $0 \leqslant z \leqslant z_m$

$$|H'_{mI}| = |H'_{msI}|\left(1 - t_1\frac{z}{z_m}\right)^{2/m_1} \quad (55)$$

$$|H''_{mI}| = |H''_{msI}|\left(1 - t_1\frac{z}{z_m}\right)^{2/m_2} \quad (56)$$

(ii) for $z_m \leqslant z \leqslant z_m + z_{p\,max}$

$$|H_{mII}| = |H_{mcr}|\left(1 - t_{2\,max}\frac{z - z_m}{z_{p\,max}}\right)^{2/n} \quad (57)$$

On the other hand, on the basis of eqns. 13 and 15, we obtain:

$$|H'_{myI}| = |H'_{msyI}|\left(1 - t_1\frac{z}{z_m}\right)^{r'_1} \quad (58)$$

$$|H''_{myI}| = |H''_{msyI}|\left(1 - t_1\frac{z}{z_m}\right)^{r'_2} \quad (59)$$

$$|H_{myII}| = |H_{mcr}|\left(1 - t_{2\,max}\frac{z - z_m}{z_{p\,max}}\right)^{v'_{2\,max}} \quad (60)$$

The right-hand sides of eqns. 55, 56, 57 and 58, 59 and 60 should be equal. Hence, we determine real parts and next imaginary parts of characteristic roots of eqns. 17, 18 and 19. Comparing the real parts of exprs. 17, 49 and 19 and 50 we obtain equations of fourth-order with respect to the variables z_m and $z_{p\,max}$:

$$4\left(\frac{m_1}{4-m_1}\right)^2\left(\frac{z_m}{d_st_1}\right)^4\cos^2\frac{\psi_s}{1-t_1} + 2\left(\frac{z_m}{d_st_1}\right)^2 \sin\frac{\psi_s}{1-t_1} - \frac{1}{4}\left[\left(\frac{4-m_1}{m_1}\right)^2 - 1\right] = 0$$

$$4\left(\frac{n}{4-n}\right)^2\left(\frac{z_{p\,max}}{d_{max}t_{2\,max}}\right)^4\cos^2\frac{\psi_{max}}{1-t_{2\,max}} + 2\left(\frac{z_{p\,max}}{d_{max}t_{2\,max}}\right)^2 \sin\frac{\psi_{max}}{1-t_{2\,max}} - \frac{1}{4}\left[\left(\frac{4-n}{n}\right)^2 - 1\right] = 0$$

Hence, there are determined thicknesses z_m, eqn. 20, and $z_{p\,max}$, eqn. 21. A similar procedure takes place in case of $H_{msy} \leqslant H_{mcr}$ where quantities v_2, eqn. 26, and z_p, eqn. 27, are determined.